https://doi.org/10.5194/egusphere-2026-2490
Preprint. Discussion started: 21 May 2026

Predicting Aviation Contrail Occurrence Using Bayesian Population Statistics From Reanalysis Data

Daniel A. Williams[1], Cyril J. Morcrette[1,2], and James M. Haywood[1]

[1]Department of Mathematics and Statistics, University of Exeter, Exeter, UK
[2]Met Office, Exeter, EX1 3PB, UK

Correspondence: Daniel A. Williams (d.a.williams3@exeter.ac.uk)

Abstract. Despite the ongoing climate crisis and recent pandemic-induced disruption, the aviation sector is expected to experience 5% annual growth over the next decade. While the industry moves towards decarbonisation through use of sustainable fuels and improved operating practices, the contribution by non-CO2 effects become ever more apparent. Contrails and contrail-induced cirrus clouds contribute an estimated 57% to the sector's total effective radiative forcing (ERF). Contrail avoidance methods are gaining ground as tools to strategically reroute flights to reduce their ERF by predicting contrail forming regions in advance.

The task of prediction remains a challenge however, with typical methodologies employing either highly parametrised models that suffer from uncertainties, or machine learning methods that are heavily abstracted away from the background physics. We propose a novel, robust method for contrail prediction that leverages large-scale population behaviours. Using ERA-5 reanalysis and the *OpenContrails* dataset for over 50,000 confirmed contrails between 2019 and 2020 over North America, we train an informed contrail predictor using Bayesian methods which we verify on unseen data. Results and statistical evaluation of this model are presented, providing a scalable but interpretable contrail predictor with good skill ($F_1 = 0.801$) that could be run using output from numerical weather prediction models, or time-slice outputs from high-resolution climate models.

1 Introduction

The aviation sector supports a global multi-billion pound industry that continues to experience rapid growth, despite a temporary contraction during the Covid-19 pandemic (ICAO, 2023) and the ongoing backdrop of the climate crisis. Passenger and freight flows have approximately quadrupled between 1990 and 2019, with the industry having now rebounded past pre-pandemic levels (ICAO, 2024). Human-induced climate change is now an undeniable truth, with the general public understanding that it is driven predominantly by CO_2 emissions; some of which come directly from aviation activity. Despite this, with 5% per annum growth predicted over the coming decade (Vaugeois, 2019; Gössling and Humpe, 2020; Jaramillo et al., 2022), we must acknowledge that the aviation sector will continue to grow despite increased awareness of the industry's contribution towards global warming. As a result, the sector should direct efforts into reducing the climate impact of aviation as a whole.

Aviation emissions presently contribute approximately 3.5% of global anthropogenic effective radiative forcing (ERF) (Lee et al., 2009; Klöwer et al., 2021). The climate impacts associated with aviation activity can be attributed to both CO_2 and non-

https://doi.org/10.5194/egusphere-2026-2490
Preprint. Discussion started: 21 May 2026

CO_2 effects, with the effects of the former being better understood due to the products of the burning fossil-fuel hydrocarbons being CO_2 and H_2O. While many economic sectors are projected to decarbonise in future through electrification, there is no such 'silver bullet' for aviation. Electric planes are expected to provide a minor contribution to short-haul flights by 2050 along with hydrogen-powered aircraft (IATA, 2021; IEA, 2021), however both are fraught with difficulties from range limitations (Schwab et al., 2021) to logistical complications (Yusaf et al., 2022; Degirmenci et al., 2023). Significant expectation is being placed on sustainable aircraft fuels (SAFs), which are otherwise conventional aviation fuels but produced from non-fossil sources that are less carbon-intensive to produce (Bauen et al., 2020; Bergero et al., 2023).

At present, the majority of aviation ERF comes from non-CO_2 effects; the contribution from which will only increase as the sector decarbonises and places an increasing reliance upon SAFs (Gryspeerdt et al., 2024). Improved aircraft designs and fuels are actively being developed to provide more efficient flight (Saulgeot et al., 2023) and to reduce the ERF of nitrogen oxide (NO_x) emissions (Fritz et al., 2020), aerosols (black carbon and sulphates), and stratospheric water vapour (Voigt et al., 2021). Each of these nonetheless are dwarfed by the largest contribution from contrails and contrail-induced cirrus clouds (Singh et al., 2024), which provide an estimated 57% of aviation's total ERF (Lee et al., 2021).

Contrails are narrow, linear, ice clouds that form in the upper troposphere in the wake of an aircraft passing through a region of cold, humid air. The combustion of any hydrocarbon fuel (e.g. kerosene) or hydrogen produces water, which is first expelled as vapour out of the hot exhaust of a jet engine. The entrainment and mixing of cold ambient air from the upper troposphere with the exhaust plume rapidly cools the vapour, allowing the formation of ice crystals around aerosol particles (Schumann, 1996; Voigt et al., 2010; Kärcher, 2018). A contrail forms if the additional water provided from fuel combustion exceeds the local saturation vapour pressure (Schmidt, 1941; Appleman, 1953; Schumann, 1996), although ordinarily diffusion and turbulence in the wake of the aircraft will dissipate the contrail within a number of minutes. However, if ambient conditions are saturated with respect to ice, the contrail will persist (Sanogo et al., 2024), often being advected and sheared into an extended contrail-induced cirrus cloud (Duda et al., 2004; Haywood et al., 2009; Wang et al., 2024). The relatively large positive ERF provided by persistent contrails and contrail-induced cirrus arises from their interaction with radiation, capable of contributing both a short-wave (cooling) and long-wave (warming) effect. During daytime, the two effects are opposite and broadly comparable, while at night contrails provide a strong warming effect (Penner et al., 1999; Digby et al., 2021; Quaas et al., 2021; Ortiz et al., 2024), an order of magnitude higher than that due to CO_2. The relative strength of the radiative forcing from contrails is such that they are the largest contributor to aviation ERF in spite of their short lifetime (Petzold et al., 2025).

With persistent contrails and contrail-induced cirrus providing the largest contribution to aviation ERF, there is increasing interest from governments and industry towards minimising non-CO_2 radiative forcing from flights (Lee et al., 2020), particularly from contrails (Cathcart et al., 2024; Miller et al., 2024; T&E, 2025). One strategy being explored is contrail avoidance/re-routeing (Filippone, 2015; Teoh et al., 2020; Sun et al., 2024). As persistent contrails are observed only in cold, humid regions of the troposphere (Rädel and Shine, 2010), if it were possible to predict contrail-forming regions in advance of a flight, could we avoid making a contrail by subtly re-routeing the flight; thereby eliminating an additional source of non-CO_2 radiative forcing in the first place? A distinct advantage of this approach is that it need only be applied to the minority of flights that contribute disproportionately to the sector's ERF (Teoh et al., 2020). The conditions required for persistent contrails are

https://doi.org/10.5194/egusphere-2026-2490
Preprint. Discussion started: 21 May 2026

commonly found in extra-tropical regions, so transatlantic flights between Europe and North America are a key target (Gierens et al., 1999; Minnis et al., 1999; Gierens and Spichtinger, 2000; Teoh et al., 2022; Wolf et al., 2024) as well as flights over Japan (Sekine et al., 2025). Case studies have suggested that significant decreases in contrail ERF could be achieved for a marginal (0.5–2%) increase in flight duration and CO_2 forcing; resulting from the additional fuel burn required to avoid the contrail formation region (Grewe et al., 2014; Yin et al., 2018; Avila et al., 2019; Borella et al., 2024). With the clear potential for selective contrail avoidance to reduce the ERF from aviation, industry-facing tools have already been developed (Martin Frias et al., 2024; Sonabend-W et al., 2024), further demonstrating interest in this area.

A significant challenge for contrail avoidance schemes is regarding the quality and reliability of predicting where contrail-forming regions will be. One wishes to avoid diverting a flight around a predicted contrail-forming region only for the forecast to be inaccurate: not only will additional fuel have been burned, but a contrail might still form, leading to an increased total radiative forcing from the flight. At present, the task of predicting contrails is through a non-trivial combination of observational, physical, and numerical constraints (Gierens et al., 2020). Very few aircraft in the global fleet have instrumentation capable of measuring relative humidity during flight (McCausland, 2024), meaning we lack a high confidence dataset of the atmospheric conditions of contrails in situ. To overcome this, algorithms have been developed to match satellite imagery to flight data (Chevallier et al., 2023; Sarna et al., 2025), though the resolution of infra-red imagers remains a constraint due to the thin shape of contrails (Driver et al., 2025). Mannstein et al. (2010), Schumann et al. (2013) and Low et al. (2025) use ground-based imagery as an alternative, with Roosenbrand et al. (2023) leveraging this to estimate contrail height. Schumann (2012) and Schumann et al. (2012) provide a toolkit for predicting contrails, improving the ability to quantify radiative forcing of contrail-producing flights (Engberg et al., 2025). One drawback to this approach is that the micro-physics of ice clouds are notoriously complicated (Petzold et al., 2025), typically relying on parametrisations. This introduces uncertainties in prediction (Platt et al., 2024), resulting in different predictions for contrail ERF between models (Bock and Burkhardt, 2016; Zhang et al., 2025). More recently, the development of machine learning (ML) methods have enabled a variety of new approaches for contrail analysis, replacing and/or augmenting methods previously summarised by Jarry (2024): from identifying contrails in satellite (Kulik, 2019; Ng et al., 2024; Yu et al., 2024) and ground-based (Pertino et al., 2024) imagery; matching imagery with flight data (Geraedts et al., 2024); to the reconstruction of contrail height (Meijer et al., 2024).

Both traditional and ML methods have relative advantages and disadvantages to be aware of. Traditional algorithmic approaches are typically easier to understand than ML methods, with decisions and outputs in general more interpretable. They are however somewhat reliant on parametrisation schemes, of which there are significant uncertainties and variation between models for upper tropospheric water vapour and ice-cloud microphysics, leading to biases that must be accounted and corrected for. Currently only the Météo-France ARPEGE model (Arriolabengoa et al., 2025) has an explicit representation of ice supersaturation regions for contrail predictions. ML methods can overcome this barrier since a model can 'learn' any required parametrisations and these can be adjusted in the light of new data. They however often suffer from the 'black-box' problem, which industry partners and policymakers may be more reluctant to make use of if decisions cannot be adequately justified. Once trained, predictions provided by these models are quick and cheap to produce, which could be advantageous in the practical rollout of a contrail avoidance scheme. Another difficulty common to many approaches, ML and traditional alike, is the

https://doi.org/10.5194/egusphere-2026-2490
Preprint. Discussion started: 21 May 2026

requirement to match observed contrails to real flight data at some stage in the analysis. This is a non-trivial task, especially since contrail height cannot be easily elucidated from imagery. Flight data availability provides an additional complication, being typically only available for a certain time window and often having to be explicitly requested at financial cost.

We propose a new method that aims to provide a toolkit to overcome some of the above issues, blending the scalability and ease of calculation of ML methods, with the robust scientific explainability of a traditional statistical method. In the absence of a widespread database of suitable in-flight relative humidity measurements, rather than attempting to use algorithms or ML methods to match contrails explicitly to flight data, we leverage the behaviour of large-population statistics applied to a known database of confirmed contrails and a reanalysis dataset. Using this, we learn the meteorological conditions associated with contrail formation and, through application of Bayesian methods, we construct a simple predictive tool for contrail occurrence at a given humidity and pressure height. Herein we describe how the statistical predictor is constructed from a combination of reanalysis and labelled satellite data.

2 Methods

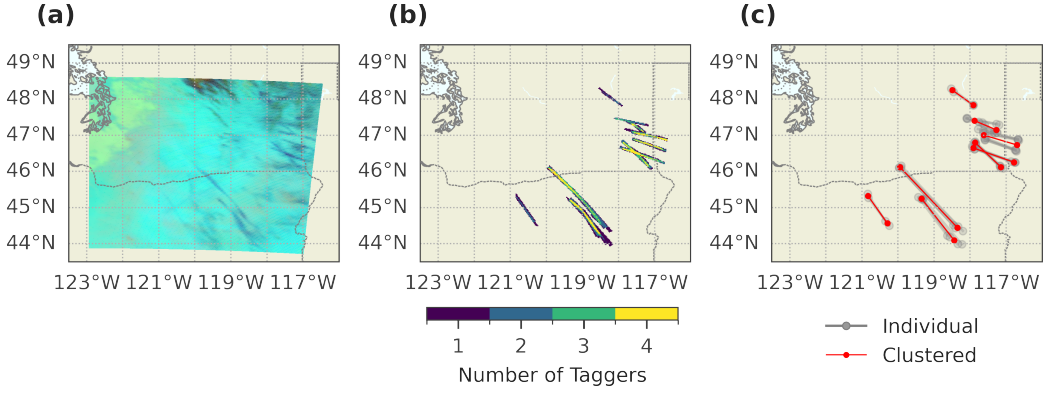

Figure 1. Example pipeline showing identification of extractable contrails from satellite imagery: (a) false-colour multi-band GOES-16 image using the ash colour scheme (Kulik, 2019); (b) contrails tagged by individual human labellers in the Open Contrails (Ng et al., 2024) dataset; (c) contrails identified from the human-tagged data, using our algorithm to provide start/end locations.

To construct a predictor for contrail occurrence, we first need to understand the meteorological conditions associated with previously confirmed contrails. To achieve this, we leverage *OpenContrails* (Google Research, 2024) to provide a ground-truth dataset of contrails that have tagged and verified by humans. *OpenContrails* contains multi-band imagery from the GOES-16 Advanced Baseline Imager (ABI) between April 2019 and April 2020. Images included in the dataset are pre-filtered according to criteria set out in Ng et al. (2024), ensuring that each tagged contrail had an associated real flight path. The authors' intention, as demonstrated, was to use this tagged dataset to train an ML model to identify contrails from satellite imagery, similar to previous efforts by McCloskey et al. (2021) and Gourgue et al. (2025). *OpenContrails* provides a total of

https://doi.org/10.5194/egusphere-2026-2490
Preprint. Discussion started: 21 May 2026

20088 training images, with a further 1879 as a validation set. Given that contrails are not often found in isolation, images likely contain multiple contrails, providing a very large dataset from which to learn population level statistics. For our meteorological data, we use hourly, $0.25°$ resolution, pressure-level relative humidity data from ERA-5 reanalysis produced by the European Centre for Medium-Range Weather Forecasts (ECMWF) (Hersbach et al., 2020). ERA-5 data is extracted between the 1000–100 hPa pressure heights which incorporates the troposphere—contrails do not form in the dry environment of the overlying stratosphere.

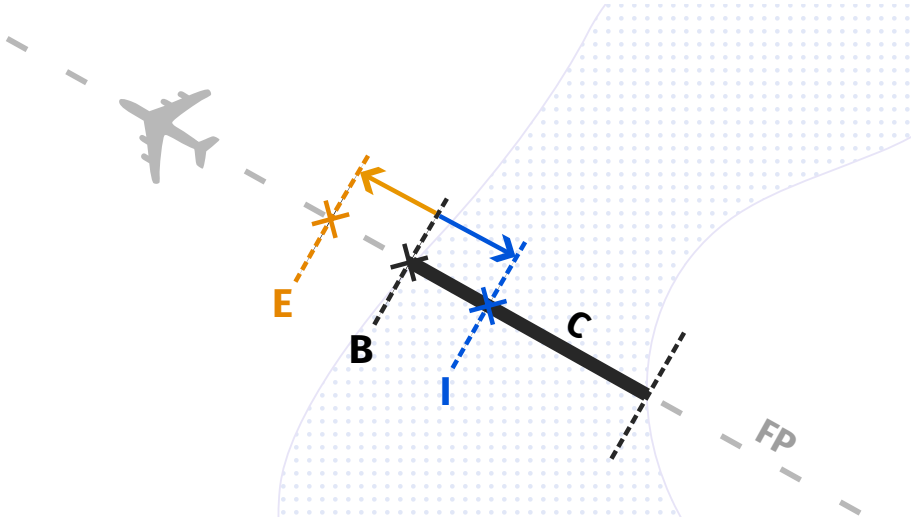

Figure 2. Schematic of contrail extraction and projection. The flight path (FP) is assumed to extend along a great-circle beyond the boundary (B) points of the contrail (C). Stippling represents a region of high relative humidity conducive to contrail formation. External (E) and internal (I) projections of the contrail boundary along the flight path are applied to both ends of contrail (only one end is demonstrated for clarity).

2.1 Contrail and Atmospheric Extraction

In addition to single-band snapshots from the GOES-16 ABI, each image in *OpenContrails* has an associated series of binarised masks, showing where a contrail has been manually labelled by each of the four individual human taggers. These masks form the basis for our initial data extraction, with the process for extracting the atmospheric conditions associated with each contrail summarised thus:

1. Geolocate dataset image, then filter to include only those within a region of interest. For our study we consider the US region, using a bounding region defined by $22.5°$N to $52.5°$N and $127.5°$W to $57.5°$W. The high levels of aviation activity in the US will provide a greater number of contrail samples.
2. For each image, iterate through contrail instance masks provided by each tagger in turn (each mask contains a single contrail). Skeletonise the feature to extract lat-lon endpoints and the principle axis.

https://doi.org/10.5194/egusphere-2026-2490
Preprint. Discussion started: 21 May 2026

3. Use the DBSCAN (Ester et al., 1996) clustering algorithm on all skeletonised vectors in an image to create a set of aggregated contrails, with the requirement that they are labelled by multiple taggers, as demonstrated in Figure 1.
4. Using the endpoints (boundary) for each aggregated identified contrail, construct the great-circle path linking them. Use the associated bearing to project a fractional distance inwards and outwards from the boundary, depicted by schematic in Figure 2. This returns a total of six lat-lon locations: two external to the contrail (E); two at the boundary (B); and two inside the contrail (I).
5. Perform linear interpolation in time and space on the ERA-5 reanalysis to provide vertical relative humidity profiles for each of these 6 locations on each contrail.

Figure 3 provides an example of the extraction algorithm, but rather than applying to specific points, demonstrates the method applied along an extrapolated flight trajectory. This provides an atmospheric cross-section of the relative humidity profile congruent with the contrail and progenitor flight path.

The extraction algorithm described above makes a number of assumptions, which when considered for a single contrail in isolation would fail to provide any substantive or meaningful deductions. We assume that any plane that creates a contrail follows an approximately linear (i.e. great-circle) trajectory either side of the boundary, ruling out marked changes in flight bearing or altitude. We assume that the flight may have passed in either direction along the contrail, as well as remaining agnostic to the height of the contrail. We also note that the contrail itself may have been advected by the large-scale flow between the time of formation and satellite observation. Clearly, for any individual flight, knowing information such as the direction of travel is vital for matching flight data with satellite imagery. When applied to over 100,000 contrail endpoints however, we not only minimise the impact of each of these assumptions, but can begin to learn population level behaviours by significantly reducing any signal-to-noise ratio.

To complement extractions of ERA-5 associated with confirmed contrail endpoints, we also perform an equally-sized stochastic sample of the reanalysis, bounding by the same spatio-temporal extent as the contrail extraction. The two very large sample sizes allow us to make powerful and robust statistical inferences about the likeliness of contrail formation for a given relative humidity by comparing the contrail-biased sample with the overall background climatology.

2.2 Statistical Inference & Predictions

By drawing biased and stochastic samples with over 100,000 members each, we can overcome much of the noise and uncertainty that plagues the consideration of any single contrail. From these we can construct relative humidity distributions for each sample, with the difference between the two showing the relative over-contribution of certain ranges of relative humidity at each pressure level. If contrails are associated with a higher relative humidity, one would expect an excess of observations in the contrail-biased sample at heights where aircraft commonly cruise. To assess this assertion, and to test the overall statistical difference between the relative humidity distributions at each height, we use the two-tailed Cramér-von Mises test (Darling, 1957; Anderson, 1962) which measures the goodness of fit between two empirical distributions: the probability distributions of relative humidity in the contrail-biased and stochastic samples. A higher test statistic indicates greater overall difference

https://doi.org/10.5194/egusphere-2026-2490
Preprint. Discussion started: 21 May 2026

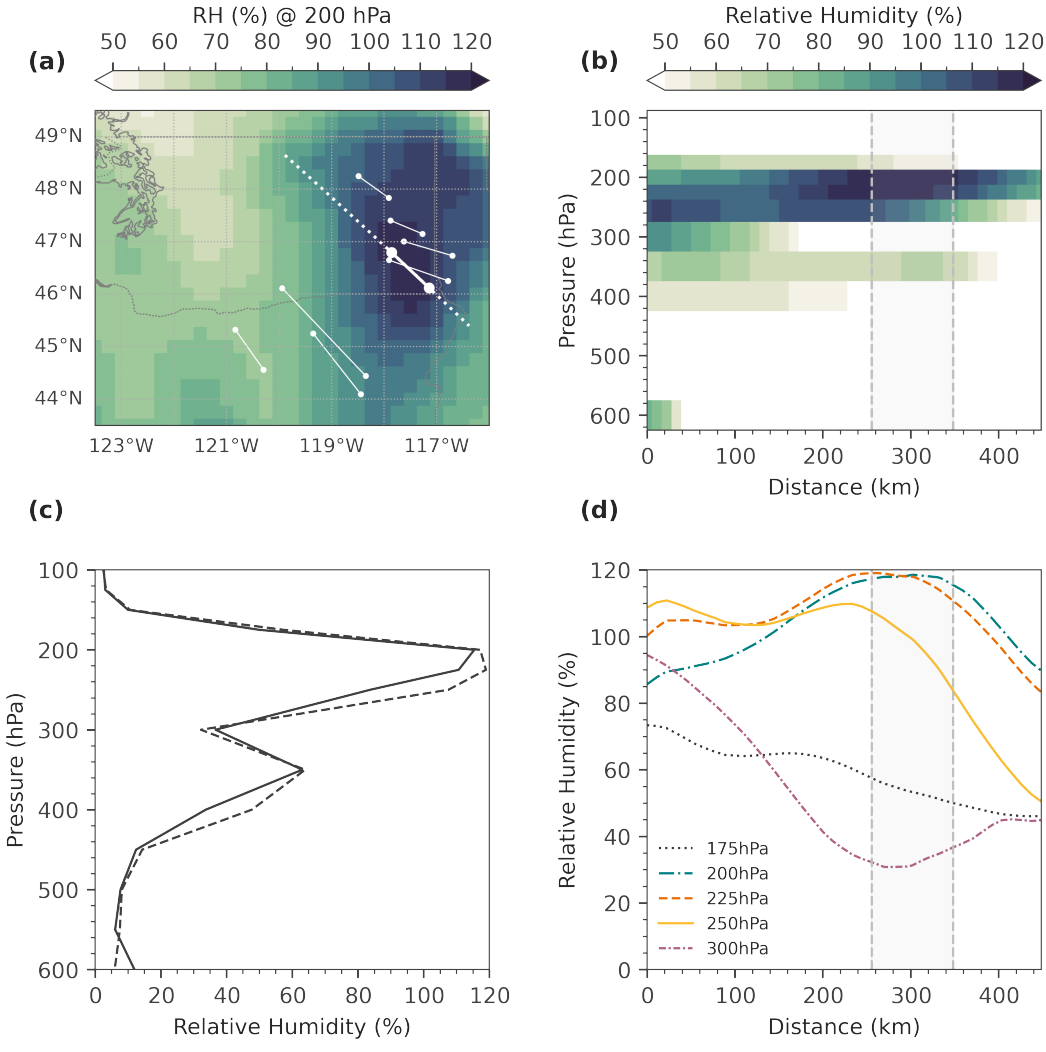

Figure 3. Extraction of ERA-5 relative humidity field for a single contrail: (a) shows relative humidity field at 200 hPa with the location of 8 contrails (thin white lines), one of which (bold white line) has been selected for data extraction. The dotted line represents a projected extension of the aircraft trajectory along a great circle; (b) provides a cross-sectional view of the upper troposphere along the projected path, with the contrail location shown by the shaded region; (c) provides vertical profiles at each contrail boundary; (d) provides a similar view to (b) but focusses on pressure levels between 175–300 hPa for easier comparison.

https://doi.org/10.5194/egusphere-2026-2490
Preprint. Discussion started: 21 May 2026

between the cumulative density function of each distribution. This test can tell us if the meteorological conditions extracted using contrail endpoints are significantly different to the background climatology. The test statistics also provide the basis for constructing a tool for contrail prediction and hence avoidance strategies.

To construct our contrail predictor, one must first learn the likeliness of contrail formation from past relative humidity data. Calculation of such a probability is not immediately trivial, but we can invoke the toolkit provided by Bayesian statistics to achieve this. The key statement of Bayesian inference is that the probability of an event A occurring given some prior knowledge B is given by

$$P(A|B) = \frac{P(B|A)\,P(A)}{P(B)}, \tag{1}$$

where $P(B|A)$ is the likelihood, $P(A)$ is the prior probability and $P(B)$ is the marginal likelihood/evidence. For our task, we can frame the probability of contrail formation given a relative humidity at each pressure level as

$$P(\text{contrail}|\text{RH}) = \frac{P(\text{RH}|\text{contrail})\,P(\text{contrail})}{P(\text{RH})}. \tag{2}$$

The likelihood is therefore the probability of a given relative humidity occurring when a contrail is present, with the prior the probability of observing a contrail and the evidence the distribution of relative humidity observed in the climatology. Using the above, the likelihood and evidence trivally follow from the existing distributions of relative humidity in the contrail-biased and stochastic samples. Choosing an appropriate prior requires additional consideration, but there are two options: a flat prior and an informed prior. A flat prior is the naïve option, assuming that contrails are equally likely to occur at any level in the atmosphere. Whilst this is simple and avoids the introduction of erroneous biases, an informed prior that encapsulates knowledge about where contrails are expected to form will provide a much better prediction; anecdotal experience tells us that contrails tend to form in the upper troposphere where the atmosphere is much colder. Since the Cramér-von Mises test provides a measure of the difference in relative humidity distributions between the contrail-biased and stochastic samples, we can use the test statistic normalised across the pressure heights as an effective proxy for the heights at which contrails are observed. This provides the informed prior for our contrail predictor, which we formulate as a 2D look-up table using ERA-5 pressure levels and relative humidity binned into 5% increments.

2.3 Model Assessment

With any predictive tool it is necessary to test the performance and accuracy of the predictions before one can trust the model. If we consider our contrail predictor as a binary classification task, the performance of such a model is conventionally assessed using a confusion matrix, which aggregates instances of an event occurring in reality versus whether it was predicted by the model. The four permutations and outcomes are summarised in Table 1.

https://doi.org/10.5194/egusphere-2026-2490
Preprint. Discussion started: 21 May 2026

Table 1. A naïve confusion matrix for contrail prediction based only on observance and prediction of contrails; before trajectory projection methods inside and outside the contrail boundary are applied along the flight path.

	Predicted	**Not Predicted**
Observed	Contrail created by flight and contrail was predicted by the model *(hit or true-positive, TP)*	Contrail created by flight but contrail was not predicted by the model *(miss or false-negative, FN)*
Not Observed	Model predicts the presence of a contrail, however no flight passed through the region to create it *(false alarm or false-positive, FP)*	Model does not predict a contrail, nor did a flight pass through the region to create one *(correct negation or true-negative, TN)*

The conventional approach to using a binary classification highlights a potential problem: whilst if a contrail is observed we know a plane has passed through that portion of atmosphere at some point prior, the corollary is not true. The absence of a contrail does not imply no plane has passed through, since it is equally possible that a plane was present but atmospheric conditions were simply not conducive to contrail formation. This apparent uncertainty can be overcome by referring back to the extrapolation-extraction method described in Section 2.1. Rather than testing predictions at the contrail endpoints, which by definition should represent a critical relative humidity threshold, we can test at the internal and external projection points. Assuming that a plane does not make drastic course deviations immediately beyond the contrail, and that relative humidity varies smoothly and monotonically near the contrail boundary, this provides our two possibilities of confirmed observation for the confusion matrix—Manshausen et al. (2022) apply an equivalent logic for the reconstruction of 'invisible' data, but rather in the context of ship track emissions.

The construction of the confusion matrix provides a visual representation of the classification task, but more typically a set of derived diagnostic values are used to quantify the model performance. The most common are precision and recall, which in turn are defined by

$$\text{Precision} = \frac{\text{TP}}{\text{TP}+\text{FP}} \qquad \text{Recall} = \frac{\text{TP}}{\text{TP}+\text{FN}}. \tag{3}$$

Precision provides the answer to "for all occasions where the model predicted a positive result, how many predictions were correct?", whilst recall answers 'for all the confirmed positive results, how many did the model correctly predict?". In turn these measures can be combined into a single metric, the F_1-score, which provides an overall measure of predictive performance and is a more robust test when classes are imbalanced. The F_1-score is given by

$$F_1 = \frac{\text{Precision} \cdot \text{Recall}}{\text{Precision}+\text{Recall}} = \frac{2\,\text{TP}}{\text{TP}+\text{FP}+\text{FN}}, \tag{4}$$

with increasing model skill indicated by a value closer to 1. By default, these binary classification metrics assume a threshold value of 0.5, however we can also test the model performance for all threshold values. The receiver-operator characteristic (ROC) curve graphically represents the true positive rate (recall) versus the false positive rate, showing the trade-off between

https://doi.org/10.5194/egusphere-2026-2490
Preprint. Discussion started: 21 May 2026

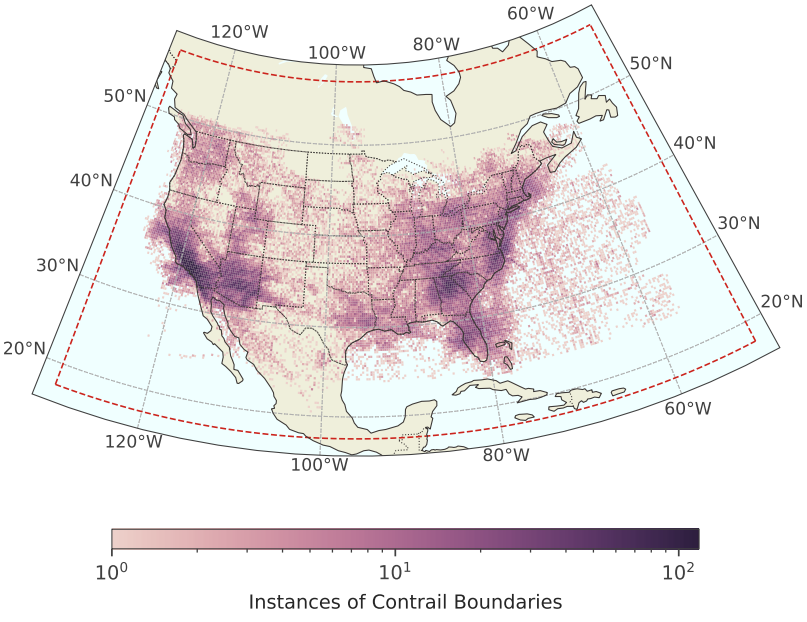

Figure 4. Distribution of extracted contrail endpoints extracted from the *OpenContrails* dataset and binned into grid cells congruent with the 0.25° ERA-5 data. A logarithmic colourmap is used to highlight lower values while the dashed red bounding box represents the spatial extent of ERA-5 data.

prioritising sensitivity or specificity in a model. A model with skill equivalent to random chance is depicted by the $y = x$ line, with well-performing models appearing above this line (Wilks, 2011). The area under the curve (AUC) quantifies how well the model can discriminate classes, with a value closer to 1 indicating better performance. ROC analysis is most useful when positive and negative classifications are equally important and the datasets are somewhat balanced (assessed with a confusion matrix). When these criteria are not satisfied, a precision-recall (PR) curve can be a more useful tool. PR curves focus more on the positive class and can handle highly imbalanced datasets; instead interrogating whether positive predictions are correct.

3 Results

Our extraction algorithm provides over 100,000 contrail-endpoints from the *OpenContrails* dataset. The distribution of these within the study area are shown in Figure 4, with high occurrence rates observed over the states of California, Georgia and also the eastern US coast. Bands representing key fly-ways between these regions (e.g. California to Florida) can be identified, corresponding to inter-state flights between major cities and aviation transport hubs. The results support the expectation that busier flight routes will have a greater incidence of contrail occurrence (*cf.* Ng et al. (2024, Figure 16)). Other regions have a much sparser distribution of extracted contrail endpoints, namely over the US mid-west, parts of the Rocky Mountains and outwards into the North Atlantic. The former two can be partly explained due to the lower population density of the underlying

https://doi.org/10.5194/egusphere-2026-2490
Preprint. Discussion started: 21 May 2026

states, from which lower aviation activity results. Unlike the mid-west and Rocky Mountains, no short-haul flights are expected to travel into the North Atlantic region, where any observed contrails are likely due to long-haul trans-Atlantic flight activity. Regions of the map that do not show instances of extracted contrail boundaries are not necessarily contrail-free: either no images from these regions are present in *OpenContrails*; or our detection algorithm did not tag any, for example if a contrail was only identified by a single human tagger. With a sample size as large as ours, the absence of data from these regions does not prevent us from learning population-level behaviours.

Figure 4 shows the locations of each of our contrail-biased sample locations. Along with the equally-sized stochastic samples, we can construct distributions of the vertical relative humidity profiles for each ERA-5 pressure level in turn. The results for a select number of pressure levels are shown in Figure 5, with relative humidity being binned into 5% intervals up to 165%. In addition to distributions for the contrail-biased and stochastic samples of relative humidity, the differences between the two are also plotted. Considering first the contrail-biased samples, we see a large variation in observed relative humidity along the vertical profile. Lower in the troposphere RH is skewed slightly towards drier conditions. At heights generally associated with aircraft cruising flight levels (300–200 hPa), there is a strong negative skew, with a sharp peak in observed RH around 100%. Higher still and the distribution flips towards dry conditions, explained by the transition through the tropopause into the dry stratosphere. For the stochastic samples, the general tendency is for drier conditions to be observed over moister ones, though between (400–200 hPa) a strong additional peak is observed around 100%. The peak can be explained by the contribution from contrails, or at least the conditions conducive to them, which are clearly seen when subtracting the two distributions from one another. Between 300–200 hPa, there is a strong oversampling of moister conditions in the biased sample versus climatology. From this we infer the average state associated with contrail observation is moister than the background state, which is supported by the theory behind contrail and ice-cloud formation.

Figure 6 shows the results from the two-tailed Cramér-von Mises test, which takes the distributions at each pressure height for the biased and random sample. The p-values for all pressure heights sit near the 5σ significance level, indicating that in general there is a clear difference between the conditions associated with contrails and a random sample. The test statistic peaks around 200–250 hPa, confirming that this range of pressure heights is where the contrail-biased and stochastic samples of relative humidity are most different. One powerful deduction that can be made from the test statistic is that by using population-level statistics, we have effectively reconstructed the heights at which contrails appear despite having no direct information about the height of observed contrails nor individually matched flight paths. The assertion that contrails typically form between 200–250 hPa is reasonable given this corresponds to the upper-most levels of the troposphere, where temperatures are commonly below -40°C—the threshold for pure ice-phase clouds—and the saturation vapour pressure is very low. By normalising the test statistic distribution across pressure levels, we construct a statistically-grounded derived prior that may be used to improve a contrail predictor.

Using Bayes theorem we can now calculate contrail formation probabilities with our predictive tool set out in Equation 2. Two versions are provided: 1) uses a flat prior that assumes naïvely that contrails can form at any height in the atmosphere; 2) uses the informed prior constructed using the results from the CVM test. The matrix of these predictions are shown in Figure 7. When the flat prior is use, nearly all combinations of input humidity-pressure have negligible probability of producing a

https://doi.org/10.5194/egusphere-2026-2490
Preprint. Discussion started: 21 May 2026

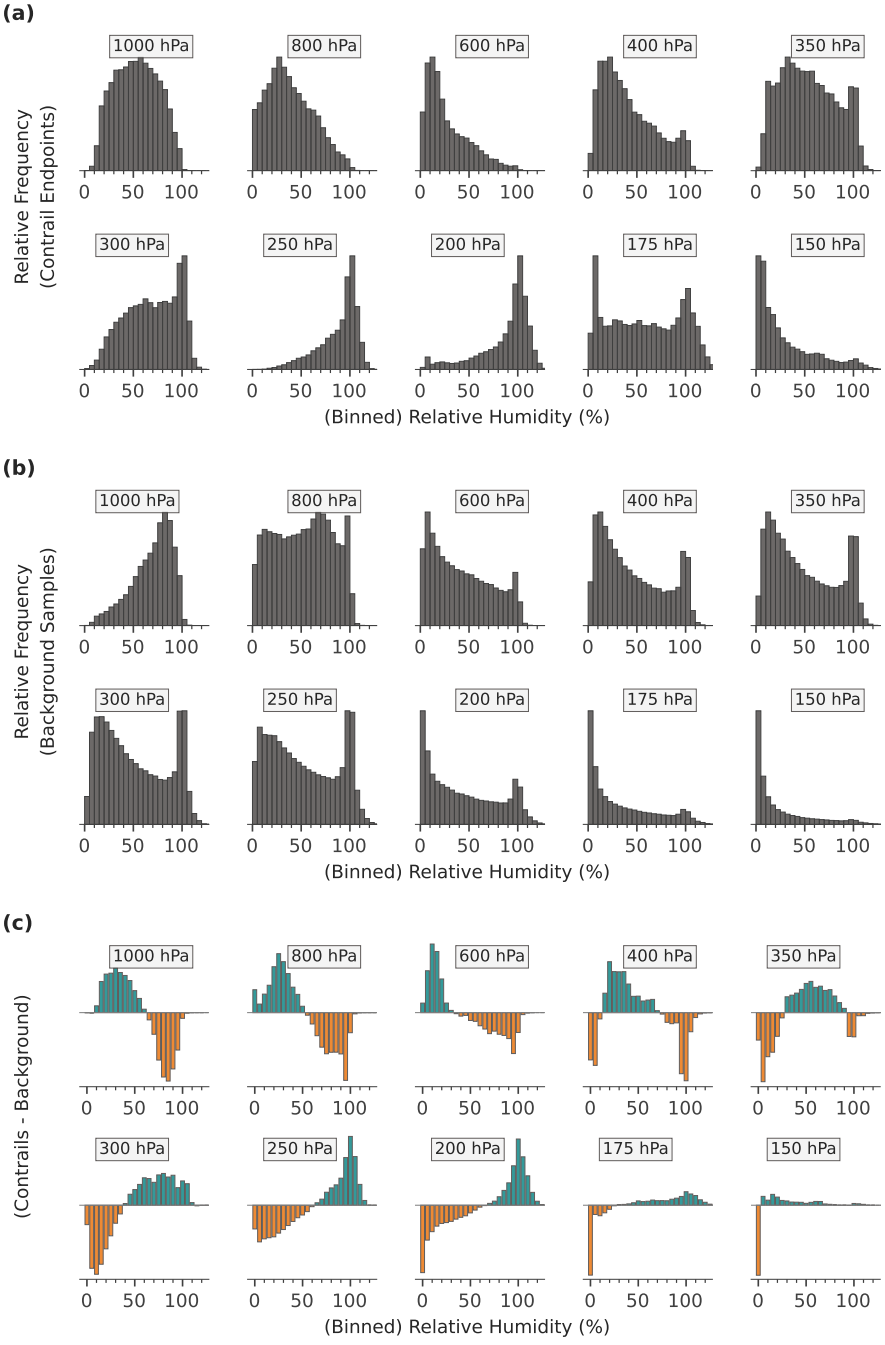

Figure 5. Distributions of sampled binned relative humidity at 12 ERA-5 pressure levels: (a) for extracted contrail endpoints; (b) for stochastic sampling of domain; (c) difference between the two distributions. Total number of samples in each histogram is equal, with values on y-axis hidden since each distribution is normalised by the maximum value.

https://doi.org/10.5194/egusphere-2026-2490
Preprint. Discussion started: 21 May 2026

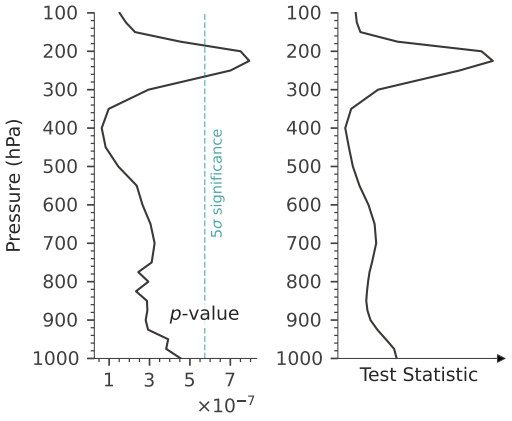

Figure 6. Results from the Cramér-von Mises test between a contrail-biased and stochastic sample of relative humidity in ERA-5 for over 100,000 individual samples. *Left:* p-value of CVM test, with dashed blue line representing 5σ significance. *Right:* CVM test statistic, explicitly presented without values since they do not have useful relevance here—the normalised form of the distribution is provided as the informed prior distribution.

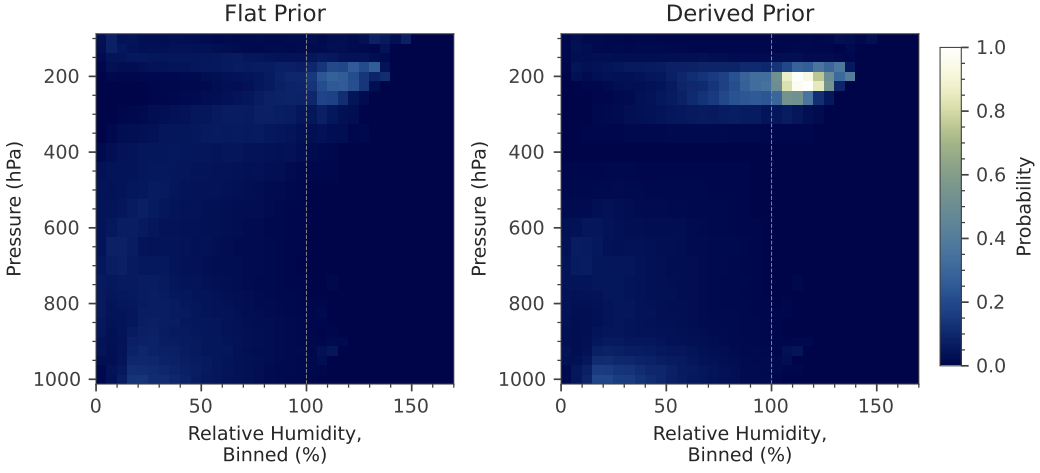

Figure 7. Comparison of the contrail predictor look-up table using a flat (left) and informed (right) prior. For each 5% relative humidity bin and ERA-5 pressure level, the colour depicts the probability of contrail formation should an aircraft pass through such a parcel of air.

https://doi.org/10.5194/egusphere-2026-2490
Preprint. Discussion started: 21 May 2026

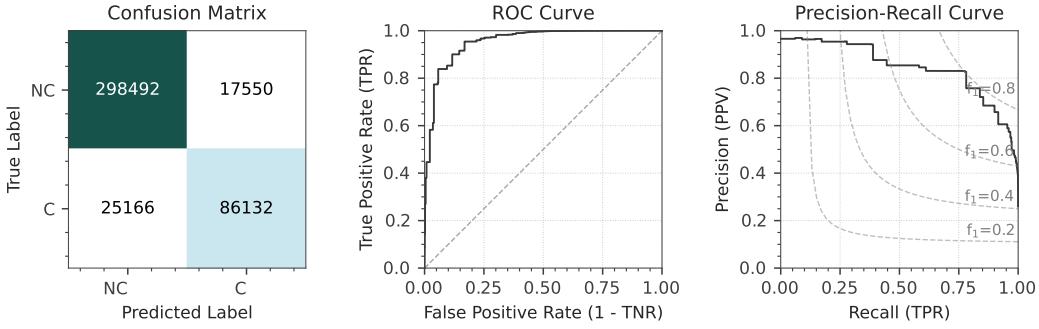

Figure 8. Quantitative assessment of the contrail predictor as a classification task. *Left*: Confusion matrix for contrail predictions versus projected observations. The labels C and NC represent contrails being predicted or not predicted. *Middle*: The Receiver-Operator Characteric (ROC) curve for binary classification as the threshold value is swept between 0 and 1. *Right*: The precision-recall curve, again as the binary threshold sweeps between 0 and 1.

contrail. The highest predicted probabilities are found in a region over 100% humidity between 175–275 hPa, but even then only peaking at approximately $p = 0.3$. With an informed prior, the contrail formation probabilities are significantly improved. While most input values retain a negligible formation probability, especially in the lower troposphere, a distinct peak appears in the upper troposphere in conditions where RH exceeds 100%. For example, a plane at 225 hPa that passes through a region of 115% RH has an almost certain chance ($p = 0.99$) of producing a contrail. Compared to the flat prior, this seems a far more realistic prediction.

Now in possession of a contrail prediction lookup-table, let us assess the performance of the classification task against a number of established metrics. The cruising altitude of aircraft, especially for transatlantic flights, is typically between flight levels FL290 and FL410; corresponding to a pressure range of approximately 300 and 200 hPa respectively. The confusion matrix for classification predictions between these heights are shown in Figure 8. As noted earlier in Section 2.1, if no contrail is observed in a satellite image, that does not mean that a contrail could not have formed; it may simply be that no aircraft has passed through the region so none could be created. The flight projection method previously described however can overcome this limitation, allowing the four permutations of predicted versus classifications to be constructed. The confusion matrix shows that the dominant class is one where neither the model predicted a contrail, nor was one observed. Given the sky is not littered with contrails at all times, this makes intuitive sense as many satellite images will likely not contain any contrails. The second largest class are contrails that were observed and also predicted by the model, which arguably are the greatest initial indicator of model success. This category is more than three times larger than either of the false classifications, providing values of precision $= 0.831$, recall $= 0.774$, and $\mathrm{F}_1 = 0.801$. The two other classes represent failure cases where a contrail is observed but not forecast, or forecast but not observed.

These results indicate a well-behaving model, which is additionally verified by the ROC curve in Figure 8. The curve is much higher than the $y = x$ line (which denotes random skill), with an AUC close to 1. As identified by the confusion matrix

https://doi.org/10.5194/egusphere-2026-2490
Preprint. Discussion started: 21 May 2026

however, the classifications are highly mismatched in size, so ROC is not the most useful graphical metric. The result for the precision-recall curve, which deals better with imbalanced classifications, shows the model's skill remains robust with a high level of skill. These results provide confidence that the contrail predictor does reasonably well at predicting whether contrails should be observed for a given set of input parameters. These quantitative results, whilst mathematically grounded, are not the most interpretable; how can one convince oneself that the model is really working, perhaps with a more qualitative result?

The original model was trained on 20088 images from the *OpenContrails* dataset. In addition to the training images there is a smaller set of 1879 validation images that were unseen in the development of the probability look-up table. If we take the geolocated timestamp of one of these images, extract the matching ERA-5 RH field and pass it through the look-up table, one can produce an array corresponding to the predicted contrail probability when the satellite image was taken. If one selects a single pressure level, this produces a contrail formation probability map; the results of which for three satellite images are shown in Figure 9. In each of the three examples, the region of high contrail formation likeliness coincides broadly with areas of the GOES-16 satellite imagery that show contrails (dark blue linear features). The regions don't necessarily match perfectly, however this may be explained by additional factors such the limited vertical resolution of the look-up table (in turn derived from ERA-5 limitations), or advection that moves contrails away from their original formation location by the time satellite overpass occurs.

4 Conclusions

This study introduces a statistically robust and versatile method for the development of a contrail prediction tool that leverages population-level statistics and Bayesian methods. Previous studies for contrail prediction have generally employed either highly parametrised models or poorly explainable machine learning models, each with their relative advantages and disadvantages. In comparison, we believe that we have developed a flexible tool that strikes a balance between scalability and explainability. Since the model is grounded in population-level statistical analysis, the prediction pipeline is highly explainable and derived directly from the atmospheric state, with little to no physical abstraction versus an ML model. That said, once trained and a look-up table is produced, our model is straightforward to scale up and apply like an ML model.

By requiring minimal inputs and demonstrating resilience to biases, such as those within the source ERA-5 relative humidity data (*c.f.* ice supersaturation in Teoh et al. (2022)), our approach offers a highly scalable framework that is agnostic to the data source and readily applicable across diverse atmospheric models and observational datasets. This provides a basis for on-line contrail predictions with the output from a numerical weather prediction model. Unlike many previous approaches that are reliant on commercial aviation data, which often comes with licensing and cost considerations, our technique mitigates the inherent uncertainties associated with matching exact flights by leveraging the improved signal-to-noise ratio that results from large sample sizes. This approach is particularly valuable in both research and operational settings where quality or availability of accurate flight information varies substantially, such as over the mid-Atlantic where ADS-B data is often missing.

A statistical assessment of our model shows a robust performance with good quantitative and qualitative skill. An F_1 score over 0.8 represents a model with significantly better than random skill, with the ROC and precision-recall curve providing

https://doi.org/10.5194/egusphere-2026-2490
Preprint. Discussion started: 21 May 2026

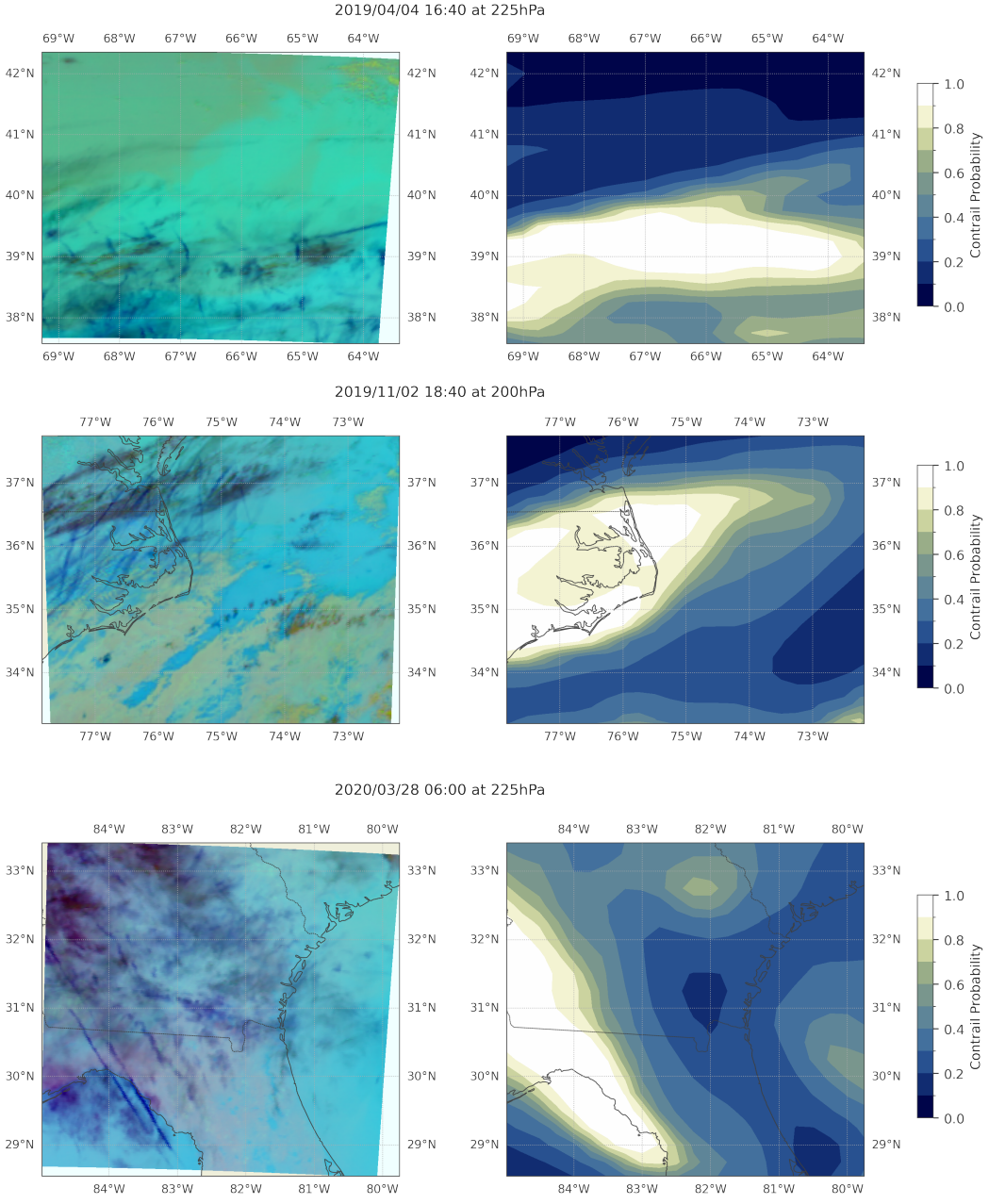

Figure 9. Comparison of three predictions from our model for contrail formation probability versus a satellite image taken at a similar time. Left panel shows composite false-colour GOES-16 image, where contrails can be identified as dark blue linear streaks. Right panel provides a modelled map of predicted contrail formation probability for a specific ERA-5 pressure level. Time, location and predicted pressure level are provided above each pair of images.

https://doi.org/10.5194/egusphere-2026-2490
Preprint. Discussion started: 21 May 2026

support to this. One should be aware of the two failure cases, which are additionally complicated by the fact that a model prediction may be correct but there was no plane to produce a contrail in the training image (or simply the model was wrong). The comparison of satellite images and corresponding contrail prediction maps in Figure 9 provides a visual demonstration of the method where statistical metrics are harder to interpret by the general reader.

We acknowledge that the model is not perfect or free from all biases. Whilst efforts have been made to consider various sources of uncertainty in the predictions, some cannot be ignored. The image selection criteria used in *OpenContrails* inherently biases observations and hence extraction of atmospheric conditions to regions where aircraft commonly fly. Atmospheric extractions from the contrail samples may therefore be slightly biased due to having little data from specific areas, however we have sought to overcome this by extracting the stochastic samples from a much larger bounding-box region that covers areas over the ocean and more sparsely populated regions. In addition, the identification of contrails by human taggers and the subsequent ML model in Ng et al. (2024) is heavily influenced by the difficulty in identifying contrails in (false-colour) satellite images. Contrails are most clearly identifiable with underlying clear-sky conditions, with challenges posed by the presence of other natural ice clouds and substantial cover by underlying cloud layers. These scenarios could lead to the oversampling of dry conditions in the lower atmosphere in the contrail-sampled extractions, however this should be a less important when considering the upper atmosphere where aircraft typically cruise. Opportunities will arise in future to refine predictions as a greater proportion of the global aviation fleet is fitted with the instrumentation to measure relative humidity in-situ, an ability limited to a select few aircraft at present. There is also scope for further development and refinement of our method, for example moving away from a dependence upon a discretised look-up table.

Our results provide a framework for development and broader adoption within research and industry. The field of contrail detection and avoidance is developing quickly, particularly with intergovernmental agencies and changes to legislation now beginning to 'cost-in' non-CO_2 aviation effects (European Parliament, 2025). As such, many competing and complementary approaches for tackling the issue should be explored. Machine learning methods are currently being tested with selected industry partners (McCloskey et al., 2023), though the most recent findings of Sankar et al. (2026) suggest that whilst predictions are likely sound, there is an additional challenge to face in the form of human decision making. In that study, flight controllers avoided supplying a contrail avoidance routeing to pilots 85% of the time, with only 60% of such routeings actually being flown, suggesting there is a strong psychological element. Whether this is due to perceived superior knowledge of flight controllers or mistrust of AI (or other reasons) is beyond the scope of our work. By offering a method for contrail prediction that is highly explainable, interpretable and scalable, we believe there is scope to help overcome issues regarding the adoption of contrail avoidance methods. This study therefore contributes to the wider societal goal of using technical innovations to mitigate contrail radiative forcing—thereby human-driven climate change—in an area that is often fraught with disagreements between economics and policy.

https://doi.org/10.5194/egusphere-2026-2490
Preprint. Discussion started: 21 May 2026

Code availability. Analytical code and notebooks used in this project can be accessed on a GitHub repository (https://github.com/daw538/williams2026-contrails). Third-party source data for *OpenContrails* is accessible from Google Cloud Storage at gs://goes_contrails_dataset whilst ERA-5 data can be downloaded from the Copernicus Climate Data Store (CDS).

Author contributions. Conceptualisation: DAW, CJM, JMH; Data curation: DAW; Formal analysis: DAW; Funding acquisition: JMH; Investigation: DAW; Methodology: DAW, CJM; Project administration: CJM, JMH; Software: DAW; Supervision: CJM; Validation: DAW; Visualization: DAW; Writing - original draft: DAW Writing - review and editing: DAW, CJM, JMH.

Competing interests. The authors declare that they have no conflict of interest.

Acknowledgements. The authors would like to thank the reviewers for their time taken to comment on this manuscript, and also to the editor. We also acknowledge funding from NERC as part of the project Quantifying and Reducing aviation Contrail radiative forcing (QR-CODE) (Chen et al., 2024), NE/Z503800/1.

https://doi.org/10.5194/egusphere-2026-2490
Preprint. Discussion started: 21 May 2026

References

Anderson, T. W.: On the Distribution of the Two-Sample Cramer-von Mises Criterion, The Annals of Mathematical Statistics, 33, 1148–1159, https://doi.org/10.1214/aoms/1177704477, 1962.

Appleman, H.: The Formation of Exhaust Condensation Trails by Jet Aircraft, Bulletin of the American Meteorological Society, 34, 14–20, https://doi.org/10.1175/1520-0477-34.1.14, 1953.

Arriolabengoa, S., Crispel, P., Jaron, O., Bouteloup, Y., Vié, B., Li, Y., Petzold, A., and Plu, M.: Modeling and Verifying Ice Supersaturated Regions in the ARPEGE Model for Persistent Contrail Forecast, Atmospheric Chemistry and Physics, 25, 18 051–18 076, https://doi.org/10.5194/acp-25-18051-2025, 2025.

Avila, D., Sherry, L., and Thompson, T.: Reducing Global Warming by Airline Contrail Avoidance: A Case Study of Annual Benefits for the Contiguous United States, Transportation Research Interdisciplinary Perspectives, 2, 100 033, https://doi.org/10.1016/j.trip.2019.100033, 2019.

Bauen, A., Bitossi, N., German, L., Harris, A., and Leow, K.: Sustainable Aviation Fuels : Status, Challenges and Prospects of Drop-in Liquid Fuels, Hydrogen and Electrification in Aviation, Johnson Matthey Technology Review, 64, 263–278, https://doi.org/10.1595/205651320X15816756012040, 2020.

Bergero, C., Gosnell, G., Gielen, D., Kang, S., Bazilian, M., and Davis, S. J.: Pathways to Net-Zero Emissions from Aviation, Nature Sustainability, 6, 404–414, https://doi.org/10.1038/s41893-022-01046-9, 2023.

Bock, L. and Burkhardt, U.: Reassessing Properties and Radiative Forcing of Contrail Cirrus Using a Climate Model, Journal of Geophysical Research: Atmospheres, 121, 9717–9736, https://doi.org/10.1002/2016JD025112, 2016.

Borella, A., Boucher, O., Shine, K. P., Stettler, M., Tanaka, K., Teoh, R., and Bellouin, N.: The Importance of an Informed Choice of CO_2-Equivalence Metrics for Contrail Avoidance, Atmospheric Chemistry and Physics, 24, 9401–9417, https://doi.org/10.5194/acp-24-9401-2024, 2024.

Cathcart, J., Andrews, S., Chen, A., Cornec, H., Kumar, S., Majholm, J., Meijers, M., Meijers, N., Miller, R., Mukhopadhaya, J., Sachdeva, N., Shapiro, M., Stern, C., and Wendling, Z. A.: Understanding Contrail Management: Opportunities, Challenges, and Insights, Tech. rep., RMI, 2024.

Chen, Y., Bellouin, N., Wang, Y., Haywood, J., and Morcrette, C.: Quantifying and Reducing Aviation Contrail Radiative Forcing (QR-CODE), https://gotw.nerc.ac.uk/list_full.asp?pcode=NE%2FZ503800%2F1&cookieConsent=A, 2024.

Chevallier, R., Shapiro, M., Engberg, Z., Soler, M., and Delahaye, D.: Linear Contrails Detection, Tracking and Matching with Aircraft Using Geostationary Satellite and Air Traffic Data, Aerospace, 10, 578, https://doi.org/10.3390/aerospace10070578, 2023.

Darling, D. A.: The Kolmogorov-Smirnov, Cramér-von Mises Tests, The Annals of Mathematical Statistics, 28, 823–838, 1957.

Degirmenci, H., Uludag, A., Ekici, S., and Karakoc, T. H.: Challenges, Prospects and Potential Future Orientation of Hydrogen Aviation and the Airport Hydrogen Supply Network: A State-of-Art Review, Progress in Aerospace Sciences, 141, 100 923, https://doi.org/10.1016/j.paerosci.2023.100923, 2023.

Digby, R. A. R., Gillett, N. P., Monahan, A. H., and Cole, J. N. S.: An Observational Constraint on Aviation-Induced Cirrus From the COVID-19-Induced Flight Disruption, Geophysical Research Letters, 48, e2021GL095 882, https://doi.org/10.1029/2021GL095882, 2021.

Driver, O. G. A., Stettler, M. E. J., and Gryspeerdt, E.: Factors Limiting Contrail Detection in Satellite Imagery, Atmospheric Measurement Techniques, 18, 1115–1134, https://doi.org/10.5194/amt-18-1115-2025, 2025.

https://doi.org/10.5194/egusphere-2026-2490
Preprint. Discussion started: 21 May 2026

Duda, D. P., Minnis, P., Nguyen, L., and Palikonda, R.: A Case Study of the Development of Contrail Clusters over the Great Lakes, Journal of the Atmospheric Sciences, 61, 1132–1146, https://doi.org/10.1175/1520-0469(2004)061<1132:ACSOTD>2.0.CO;2, 2004.

Engberg, Z., Teoh, R., Abbott, T., Dean, T., Stettler, M. E. J., and Shapiro, M. L.: Forecasting Contrail Climate Forcing for Flight Planning and Air Traffic Management Applications: The CocipGrid Model in Pycontrails 0.51.0, Geoscientific Model Development, 18, 253–286, https://doi.org/10.5194/gmd-18-253-2025, 2025.

Ester, M., Kriegel, H.-P., Sander, J., and Xu, X.: A Density-Based Algorithm for Discovering Clusters in Large Spatial Databases with Noise, in: International Conference on Knowledge Discovery & Data Mining, pp. 226–231, AAAI Press, California, ISBN 978-1-57735-004-0, https://doi.org/10.1.1.121.9220, 1996.

European Parliament: Commission Implementing Regulation (EU) 2018/2066 of 19 December 2018 on the Monitoring and Reporting of Greenhouse Gas Emissions Pursuant to Directive 2003/87/EC of the European Parliament and of the Council and Amending Commission Regulation (EU) No 601/2012 (Text with EEA Relevance), 2025.

Filippone, A.: Assessment of Aircraft Contrail Avoidance Strategies, Journal of Aircraft, 52, 872–877, https://doi.org/10.2514/1.C033176, 2015.

Fritz, T. M., Eastham, S. D., Speth, R. L., and Barrett, S. R. H.: The Role of Plume-Scale Processes in Long-Term Impacts of Aircraft Emissions, Atmospheric Chemistry and Physics, 20, 5697–5727, https://doi.org/10.5194/acp-20-5697-2020, 2020.

Geraedts, S., Brand, E., Dean, T. R., Eastham, S., Elkin, C., Engberg, Z., Hager, U., Langmore, I., McCloskey, K., Yue-Hei Ng, J., Platt, J. C., Sankar, T., Sarna, A., Shapiro, M., and Goyal, N.: A Scalable System to Measure Contrail Formation on a Per-Flight Basis, Environmental Research Communications, 6, 015 008, https://doi.org/10.1088/2515-7620/ad11ab, 2024.

Gierens, K. and Spichtinger, P.: On the Size Distribution of Ice-Supersaturated Regions in the Upper Troposphere and Lowermost Stratosphere, Annales Geophysicae, 18, 499–504, https://doi.org/10.1007/s00585-000-0499-7, 2000.

Gierens, K., Sausen, R., and Schumann, U.: A Diagnostic Study of the Global Distribution of Contrails Part II: Future Air Traffic Scenarios, Theoretical and Applied Climatology, 63, 1–9, https://doi.org/10.1007/s007040050087, 1999.

Gierens, K., Matthes, S., and Rohs, S.: How Well Can Persistent Contrails Be Predicted?, Aerospace, 7, 169, https://doi.org/10.3390/aerospace7120169, 2020.

Google Research: OpenContrails, 2024.

Gössling, S. and Humpe, A.: The Global Scale, Distribution and Growth of Aviation: Implications for Climate Change, Global Environmental Change, 65, 102 194, https://doi.org/10.1016/j.gloenvcha.2020.102194, 2020.

Gourgue, N., Boucher, O., and Barthès, L.: A Dataset of Annotated Ground-Based Images for the Development of Contrail Detection Algorithms, Data in Brief, 59, 111 364, https://doi.org/10.1016/j.dib.2025.111364, 2025.

Grewe, V., Champougny, T., Matthes, S., Frömming, C., Brinkop, S., Søvde, O. A., Irvine, E. A., and Halscheidt, L.: Reduction of the Air Traffic's Contribution to Climate Change: A REACT4C Case Study, Atmospheric Environment, 94, 616–625, https://doi.org/10.1016/j.atmosenv.2014.05.059, 2014.

Gryspeerdt, E., Stettler, M. E. J., Teoh, R., Burkhardt, U., Delovski, T., Driver, O. G. A., and Painemal, D.: Operational Differences Lead to Longer Lifetimes of Satellite Detectable Contrails from More Fuel Efficient Aircraft, Environmental Research Letters, 19, 084 059, https://doi.org/10.1088/1748-9326/ad5b78, 2024.

Haywood, J. M., Allan, R. P., Bornemann, J., Forster, P. M., Francis, P. N., Milton, S., Rädel, G., Rap, A., Shine, K. P., and Thorpe, R.: A Case Study of the Radiative Forcing of Persistent Contrails Evolving into Contrail-Induced Cirrus, Journal of Geophysical Research: Atmospheres, 114, 2009JD012 650, https://doi.org/10.1029/2009JD012650, 2009.

https://doi.org/10.5194/egusphere-2026-2490
Preprint. Discussion started: 21 May 2026

Hersbach, H., Bell, B., Berrisford, P., Hirahara, S., Horányi, A., Muñoz-Sabater, J., Nicolas, J., Peubey, C., Radu, R., Schepers, D., Simmons, A., Soci, C., Abdalla, S., Abellan, X., Balsamo, G., Bechtold, P., Biavati, G., Bidlot, J., Bonavita, M., De Chiara, G., Dahlgren, P., Dee, D., Diamantakis, M., Dragani, R., Flemming, J., Forbes, R., Fuentes, M., Geer, A., Haimberger, L., Healy, S., Hogan, R. J., Hólm, E., Janisková, M., Keeley, S., Laloyaux, P., Lopez, P., Lupu, C., Radnoti, G., de Rosnay, P., Rozum, I., Vamborg, F., Villaume, S., and Thépaut, J.-N.: The ERA5 Global Reanalysis, Quarterly Journal of the Royal Meteorological Society, 146, 1999–2049, https://doi.org/10.1002/qj.3803, 2020.

IATA: Net-Zero Carbon Emissions by 2050 (Press Release), https://www.iata.org/en/pressroom/pressroom-archive/2021-releases/2021-10-04-03/, 2021.

ICAO: Effects of Novel Coronavirus (COVID-19) on Civil Aviation: Economic Impact Analysis, https://www.icao.int/economic-impacts-covid-19-civil-aviation, 2023.

ICAO: Passenger Air Traffic Surpasses Pre-Pandemic Levels, https://www.icao.int/news/passenger-air-traffic-surpasses-pre-pandemic-levels, 2024.

IEA: Net Zero by 2050, Tech. rep., IEA, Paris, 2021.

Jaramillo, P., Kahn Ribeiro, S., Newman, P., Dhar, S., Diemuodeke, O. E., Kajino, T., Lee, D. S., Nugroho, S. B., Ou, X., Strømman, A. H., and Whitehead, J.: IPCC6 WR3 Chapter 10 - Transport, in: Climate Change 2022: Mitigation of Climate Change. Contribution of Working Group III to the Sixth Assessment Report of the Intergovernmental Panel on Climate Change, edited by Shukla, P. R., Skea, J., Slade, R., Al Khourdajie, A., van Diemen, R., McCollum, D., Pathak, M., Some, S., Vyas, P., Fradera, R., Belkacemi, M., Hasija, A., Lisboa, G., Luz, S., and Malley, J., pp. 1049–1160, Cambridge University Press, Cambridge, UK and New York, NY, USA, https://doi.org/10.1017/9781009157926.012, 2022.

Jarry, G.: Contrail Detection and Modelling Using Deep Learning, 2024.

Kärcher, B.: Formation and Radiative Forcing of Contrail Cirrus, Nature Communications, 9, 1824, https://doi.org/10.1038/s41467-018-04068-0, 2018.

Klöwer, M., Allen, M. R., Lee, D. S., Proud, S. R., Gallagher, L., and Skowron, A.: Quantifying Aviation's Contribution to Global Warming, Environmental Research Letters, 16, 104 027, https://doi.org/10.1088/1748-9326/ac286e, 2021.

Kulik, L.: Satellite-Based Detection of Contrails Using Deep Learning, Thesis, Massachusetts Institute of Technology, 2019.

Lee, D., Arrowsmith, S., Skowron, A., Owen, B., Sausen, R., Boucher, O., Faber, J., Marianne, L., Fuglestvedt, J., and van Wijngaarden, L.: Updated Analysis of the Non-CO2 Climate Impacts of Aviation and Potential Policy Measures Pursuant to EU Emissions Trading System Directive Article 30(4), Report, European Aviation Safety Agency, Cologne, Germany, 2020.

Lee, D. S., Fahey, D. W., Forster, P. M., Newton, P. J., Wit, R. C. N., Lim, L. L., Owen, B., and Sausen, R.: Aviation and Global Climate Change in the 21st Century, Atmospheric Environment, 43, 3520–3537, https://doi.org/10.1016/j.atmosenv.2009.04.024, 2009.

Lee, D. S., Fahey, D. W., Skowron, A., Allen, M. R., Burkhardt, U., Chen, Q., Doherty, S. J., Freeman, S., Forster, P. M., Fuglestvedt, J., Gettelman, A., De León, R. R., Lim, L. L., Lund, M. T., Millar, R. J., Owen, B., Penner, J. E., Pitari, G., Prather, M. J., Sausen, R., and Wilcox, L. J.: The Contribution of Global Aviation to Anthropogenic Climate Forcing for 2000 to 2018, Atmospheric Environment, 244, 117 834, https://doi.org/10.1016/j.atmosenv.2020.117834, 2021.

Low, J., Teoh, R., Ponsonby, J., Gryspeerdt, E., Shapiro, M., and Stettler, M. E. J.: Ground-Based Contrail Observations: Comparisons with Reanalysis Weather Data and Contrail Model Simulations, Atmospheric Measurement Techniques, 18, 37–56, https://doi.org/10.5194/amt-18-37-2025, 2025.

https://doi.org/10.5194/egusphere-2026-2490
Preprint. Discussion started: 21 May 2026

Mannstein, H., Brömser, A., and Bugliaro, L.: Ground-Based Observations for the Validation of Contrails and Cirrus Detection in Satellite Imagery, Atmospheric Measurement Techniques, 3, 655–669, https://doi.org/10.5194/amt-3-655-2010, 2010.

Manshausen, P., Watson-Parris, D., Christensen, M. W., Jalkanen, J.-P., and Stier, P.: Invisible Ship Tracks Show Large Cloud Sensitivity to Aerosol, Nature, 610, 101–106, https://doi.org/10.1038/s41586-022-05122-0, 2022.

Martin Frias, A., Shapiro, M. L., Engberg, Z., Zopp, R., Soler, M., and Stettler, M. E. J.: Feasibility of Contrail Avoidance in a Commercial Flight Planning System: An Operational Analysis, Environmental Research: Infrastructure and Sustainability, 4, 015 013, https://doi.org/10.1088/2634-4505/ad310c, 2024.

McCausland, R.: Aviation Contrails and Their Climate Effect, Tech. rep., IATA, Geneva, 2024.

McCloskey, K., Geraedts, S., Van Arsdale, C., and Brand, E.: A Human-Labeled Landsat-8 Contrails Dataset, in: Proceedings of the ICML 2021 Workshop on Tackling Climate Change with Machine Learning, Virtually, vol. 23, 2021.

McCloskey, K., Chen, S., Meijer, V. R., Ng, J. Y.-H., Davis, G., Elkin, C., Van Arsdale, C., and Geraedts, S.: Estimates of Broadband Upwelling Irradiance from GOES-16 ABI, Remote Sensing of Environment, 285, 113 376, https://doi.org/10.1016/j.rse.2022.113376, 2023.

Meijer, V. R., Eastham, S. D., Waitz, I. A., and Barrett, S. R. H.: Contrail Altitude Estimation Using GOES-16 ABI Data and Deep Learning, Atmospheric Measurement Techniques, 17, 6145–6162, https://doi.org/10.5194/amt-17-6145-2024, 2024.

Miller, R., Whittington, E., Gabra, S., Hodgson, P., Green, J., Kho, J., Smith, J., and Singh, D.: Five Years to Chart a New Future for Aviation - The 2030 Sustainable Aviation Goals, Text, University of Cambridge, Aviation Impact Accelerator, 2024.

Minnis, P., Schumann, U., Doelling, D. R., Gierens, K. M., and Fahey, D. W.: Global Distribution of Contrail Radiative Forcing, Geophysical Research Letters, 26, 1853–1856, https://doi.org/10.1029/1999GL900358, 1999.

Ng, J. Y.-H., McCloskey, K., Cui, J., Meijer, V. R., Brand, E., Sarna, A., Goyal, N., Van Arsdale, C., and Geraedts, S.: Contrail Detection on GOES-16 ABI With the OpenContrails Dataset, IEEE Transactions on Geoscience and Remote Sensing, 62, 1–14, https://doi.org/10.1109/TGRS.2023.3345226, 2024.

Ortiz, I., Dimitropoulou, E., de Buyl, P., Clerbaux, N., García-Heras, J., Jafarimoghaddam, A., Brenot, H., van Gent, J., Sievers, K., Otero, E., Loganathan, P., and Soler, M.: Satellite-Based Quantification of Contrail Radiative Forcing over Europe: A Two-Week Analysis of Aviation-Induced Climate Effects, in: SESAR Innovation Days 2024, arXiv, https://doi.org/10.48550/arXiv.2409.10166, 2024.

Penner, J. E., Lister, D., Griggs, D. J., Dokken, D. J., and McFarland, M.: Aviation and the Global Atmosphere: A Special Report of the Intergovernmental Panel on Climate Change, Cambridge University Press, ISBN 978-0-521-66300-7, 1999.

Pertino, P., Pavarino, L., Lomolino, S., Miotto, E., Cambrin, D. R., Garza, P., and Ogliari, E.: Ground-Based Contrail Detection by Means of Computer Vision Models: A Comparison Between Visible and Infrared Images, in: 2024 IEEE 8th Forum on Research and Technologies for Society and Industry Innovation (RTSI), pp. 254–259, ISSN 2687-6817, https://doi.org/10.1109/RTSI61910.2024.10761667, 2024.

Petzold, A., Khan, N. F., Li, Y., Spichtinger, P., Rohs, S., Crewell, S., Wahner, A., and Krämer, M.: Most Long-Lived Contrails Form within Cirrus Clouds with Uncertain Climate Impact, Nature Communications, 16, 9695, https://doi.org/10.1038/s41467-025-65532-2, 2025.

Platt, J. C., Shapiro, M. L., Engberg, Z., McCloskey, K., Geraedts, S., Sankar, T., Stettler, M. E. J., Teoh, R., Schumann, U., Rohs, S., Brand, E., and Van Arsdale, C.: The Effect of Uncertainty in Humidity and Model Parameters on the Prediction of Contrail Energy Forcing, Environmental Research Communications, 6, 095 015, https://doi.org/10.1088/2515-7620/ad6ee5, 2024.

Quaas, J., Gryspeerdt, E., Vautard, R., and Boucher, O.: Climate Impact of Aircraft-Induced Cirrus Assessed from Satellite Observations before and during COVID-19, Environmental Research Letters, 16, 064 051, https://doi.org/10.1088/1748-9326/abf686, 2021.

https://doi.org/10.5194/egusphere-2026-2490
Preprint. Discussion started: 21 May 2026

Rädel, G. and Shine, K. P.: Validating ECMWF Forecasts for the Occurrence of Ice Supersaturation Using Visual Observations of Persistent Contrails and Radiosonde Measurements over England, Quarterly Journal of the Royal Meteorological Society, 136, 1723–1732, https://doi.org/10.1002/qj.670, 2010.

Roosenbrand, E., Sun, J., and Hoekstra, J.: Contrail Altitude Estimation Based on Shadows Detected in Landsat Imagery: 13th SESAR Innovation Days, in: 13th SESAR Innovation Days, Seville, 2023.

Sankar, T., Dean, T., Abbott, T., Blickstein, J., Frías, A. M., Galyen, M., Grenham, R., Hodgson, P., McCloskey, K., Pechman, A., Robarge, T., Sanekommu, D., Sarna, A., Sonabend-W, A., Stettler, M., Zopp, R., and Geraedts, S.: Efficacy of Scalable Airline-led Contrail Avoidance, https://doi.org/10.48550/arXiv.2603.06909, 2026.

Sanogo, S., Boucher, O., Bellouin, N., Borella, A., Wolf, K., and Rohs, S.: Variability in the Properties of the Distribution of the Relative Humidity with Respect to Ice: Implications for Contrail Formation, Atmospheric Chemistry and Physics, 24, 5495–5511, https://doi.org/10.5194/acp-24-5495-2024, 2024.

Sarna, A., Meijer, V., Chevallier, R., Duncan, A., McConnaughay, K., Geraedts, S., and McCloskey, K.: Benchmarking and Improving Algorithms for Attributing Satellite-Observed Contrails to Flights, Atmospheric Measurement Techniques, 18, 3495–3532, https://doi.org/10.5194/amt-18-3495-2025, 2025.

Saulgeot, P., Brion, V., Bonne, N., Dormy, E., and Jacquin, L.: Effects of Atmospheric Stratification and Jet Position on the Properties of Early Aircraft Contrails, Physical Review Fluids, 8, 114 702, https://doi.org/10.1103/PhysRevFluids.8.114702, 2023.

Schmidt, E.: Die entstehung von eisnebel aus den auspuffgasen von flugmotoren, Schriften der Deutschen Akademie der Luftfahrtforschung, 5, 1–15, 1941.

Schumann, U.: On Conditions for Contrail Formation from Aircraft Exhausts, Meteorologische Zeitschrift, pp. 4–23, https://doi.org/10.1127/metz/5/1996/4, 1996.

Schumann, U.: A Contrail Cirrus Prediction Model, Geoscientific Model Development, 5, 543–580, https://doi.org/10.5194/gmd-5-543-2012, 2012.

Schumann, U., Mayer, B., Graf, K., and Mannstein, H.: A Parametric Radiative Forcing Model for Contrail Cirrus, Journal of Applied Meteorology and Climatology, 51, 1391–1406, https://doi.org/10.1175/JAMC-D-11-0242.1, 2012.

Schumann, U., Hempel, R., Flentje, H., Garhammer, M., Graf, K., Kox, S., Lösslein, H., and Mayer, B.: Contrail Study with Ground-Based Cameras, Atmospheric Measurement Techniques, 6, 3597–3612, https://doi.org/10.5194/amt-6-3597-2013, 2013.

Schwab, A., Thomas, A., Bennett, J., Robertson, E., and Cary, S.: Electrification of Aircraft: Challenges, Barriers, and Potential Impacts, Tech. Rep. NREL/TP-6A20-80220, National Renewable Energy Laboratory (NREL), Golden, CO (United States), https://doi.org/10.2172/1827628, 2021.

Sekine, K., Hasegawa, T., Sun, J., and Itoh, E.: Assessing Climate Impact of Contrails: Insights from Japan's High-Density Airspace and Meteorological Conditions, in: First US-Europe Air Transportation Research & Development Symposium, Prague, 2025.

Singh, D. K., Sanyal, S., and Wuebbles, D. J.: Understanding the Role of Contrails and Contrail Cirrus in Climate Change: A Global Perspective, Atmospheric Chemistry and Physics, 24, 9219–9262, https://doi.org/10.5194/acp-24-9219-2024, 2024.

Sonabend-W, A., Elkin, C., Dean, T., Dudley, J., Ali, N., Blickstein, J., Brand, E., Broshears, B., Chen, S., Engberg, Z., Galyen, M., Geraedts, S., Goyal, N., Grenham, R., Hager, U., Hecker, D., Jany, M., McCloskey, K., Ng, J., Norris, B., Opel, F., Rothenberg, J., Sankar, T., Sanekommu, D., Sarna, A., Schütt, O., Shapiro, M., Soh, R., Van Arsdale, C., and Platt, J. C.: Feasibility Test of Per-Flight Contrail Avoidance in Commercial Aviation, Communications Engineering, 3, 184, https://doi.org/10.1038/s44172-024-00329-7, 2024.

https://doi.org/10.5194/egusphere-2026-2490
Preprint. Discussion started: 21 May 2026

Sun, J., Roosenbrand, E., Nonaka, Y., and Itoh, E.: Contrail Formation and Mitigation in the Japanese Airspace: International Conference on Research in Air Transportation, Proceedings International Conference on Research in Air Transportation, 2024.

T&E: Contrail Avoidance: Aviation's Climate Opportunity of the Decade, https://www.transportenvironment.org/articles/contrail-avoidance, 2025.

Teoh, R., Schumann, U., Majumdar, A., and Stettler, M. E. J.: Mitigating the Climate Forcing of Aircraft Contrails by Small-Scale Diversions and Technology Adoption, Environmental Science & Technology, 54, 2941–2950, https://doi.org/10.1021/acs.est.9b05608, 2020.

Teoh, R., Schumann, U., Gryspeerdt, E., Shapiro, M., Molloy, J., Koudis, G., Voigt, C., and Stettler, M. E. J.: Aviation Contrail Climate Effects in the North Atlantic from 2016 to 2021, Atmospheric Chemistry and Physics, 22, 10 919–10 935, https://doi.org/10.5194/acp-22-10919-2022, 2022.

Vaugeois, M.: International Civil Aviation Organization (ICAO), in: Research Handbook on the European Union and International Organizations, chap. Research Handbook on the European Union and International Organizations, pp. 222–239, Edward Elgar Publishing, ISBN 978-1-78643-893-5, 2019.

Voigt, C., Schumann, U., Jurkat, T., Schäuble, D., Schlager, H., Petzold, A., Gayet, J.-F., Krämer, M., Schneider, J., Borrmann, S., Schmale, J., Jessberger, P., Hamburger, T., Lichtenstern, M., Scheibe, M., Gourbeyre, C., Meyer, J., Kübbeler, M., Frey, W., Kalesse, H., Butler, T., Lawrence, M. G., Holzäpfel, F., Arnold, F., Wendisch, M., Döpelheuer, A., Gottschaldt, K., Baumann, R., Zöger, M., Sölch, I., Rautenhaus, M., and Dörnbrack, A.: In-Situ Observations of Young Contrails – Overview and Selected Results from the CONCERT Campaign, Atmospheric Chemistry and Physics, 10, 9039–9056, https://doi.org/10.5194/acp-10-9039-2010, 2010.

Voigt, C., Kleine, J., Sauer, D., Moore, R. H., Bräuer, T., Le Clercq, P., Kaufmann, S., Scheibe, M., Jurkat-Witschas, T., Aigner, M., Bauder, U., Boose, Y., Borrmann, S., Crosbie, E., Diskin, G. S., DiGangi, J., Hahn, V., Heckl, C., Huber, F., Nowak, J. B., Rapp, M., Rauch, B., Robinson, C., Schripp, T., Shook, M., Winstead, E., Ziemba, L., Schlager, H., and Anderson, B. E.: Cleaner Burning Aviation Fuels Can Reduce Contrail Cloudiness, Communications Earth & Environment, 2, 114, https://doi.org/10.1038/s43247-021-00174-y, 2021.

Wang, X., Wolf, K., Boucher, O., and Bellouin, N.: Radiative Effect of Two Contrail Cirrus Outbreaks Over Western Europe Estimated Using Geostationary Satellite Observations and Radiative Transfer Calculations, Geophysical Research Letters, 51, e2024GL108 452, https://doi.org/10.1029/2024GL108452, 2024.

Wilks, D. S.: Statistical Methods in the Atmospheric Sciences, Academic Press, ISBN 978-0-12-385023-2, 2011.

Wolf, K., Bellouin, N., and Boucher, O.: Distribution and Morphology of Non-Persistent Contrail and Persistent Contrail Formation Areas in ERA5, Atmospheric Chemistry and Physics, 24, 5009–5024, https://doi.org/10.5194/acp-24-5009-2024, 2024.

Yin, F., Grewe, V., Frömming, C., and Yamashita, H.: Impact on Flight Trajectory Characteristics When Avoiding the Formation of Persistent Contrails for Transatlantic Flights, Transportation Research Part D: Transport and Environment, 65, 466–484, https://doi.org/10.1016/j.trd.2018.09.017, 2018.

Yu, J., Zhou, X., Li, L., Gao, L., Li, X., Pan, W., Ni, X., Wang, Q., and Chen, F.: High-Resolution Thermal Infrared Contrails Images Identification and Classification Method Based on SDGSAT-1, International Journal of Applied Earth Observation and Geoinformation, 131, 103 980, https://doi.org/10.1016/j.jag.2024.103980, 2024.

Yusaf, T., Fernandes, L., Abu Talib, A. R., Altarazi, Y. S. M., Alrefae, W., Kadirgama, K., Ramasamy, D., Jayasuriya, A., Brown, G., Mamat, R., Dhahad, H. A., Benedict, F., and Laimon, M.: Sustainable Aviation—Hydrogen Is the Future, Sustainability, 14, 548, https://doi.org/10.3390/su14010548, 2022.

https://doi.org/10.5194/egusphere-2026-2490
Preprint. Discussion started: 21 May 2026

Zhang, W., Van Weverberg, K., Morcrette, C. J., Feng, W., Furtado, K., Field, P. R., Chen, C.-C., Gettelman, A., Forster, P. M., Marsh, D. R., and Rap, A.: Impact of Host Climate Model on Contrail Cirrus Effective Radiative Forcing Estimates, Atmospheric Chemistry and Physics, 25, 473–489, https://doi.org/10.5194/acp-25-473-2025, 2025.